



OPEN ACCESS

EDITED BY

Sean Forbes,
University of Florida, United States

REVIEWED BY

Jun Tanihata,
Jikei University School of Medicine, Japan
Robert Grange,
Virginia Tech, United States

*CORRESPONDENCE

Hongmei Ren,
✉ hongmei.ren@wright.edu

RECEIVED 06 September 2024

ACCEPTED 28 October 2024

PUBLISHED 12 November 2024

CITATION

Brown A, Morris B, Kamau JK, Rakoczy RJ,
Finck BN, Wyatt CN and Ren H (2024) Lipin1
as a therapeutic target for respiratory
insufficiency of duchenne muscular
dystrophy.
Front. Physiol. 15:1477976.
doi: 10.3389/fphys.2024.1477976

COPYRIGHT

© 2024 Brown, Morris, Kamau, Rakoczy,
Finck, Wyatt and Ren. This is an open-access
article distributed under the terms of the
[Creative Commons Attribution License \(CC
BY\)](#). The use, distribution or reproduction in
other forums is permitted, provided the
original author(s) and the copyright owner(s)
are credited and that the original publication
in this journal is cited, in accordance with
accepted academic practice. No use,
distribution or reproduction is permitted
which does not comply with these terms.

Lipin1 as a therapeutic target for respiratory insufficiency of duchenne muscular dystrophy

Alexandra Brown¹, Brooklyn Morris¹, John Karanja Kamau¹,
Ryan J. Rakoczy², Brian N. Finck³, Christopher N. Wyatt² and
Hongmei Ren^{1*}

¹Department of Biochemistry and Molecular Biology, Wright State University, Dayton, OH, United States, ²Department of Neuroscience, Cell Biology and Physiology, Wright State University, Dayton, OH, United States, ³Division of Nutritional Science and Obesity Medicine, Washington University School of Medicine in St. Louis, St. Louis, MO, United States

In Duchenne muscular dystrophy (DMD), diaphragm muscle dysfunction results in respiratory insufficiency which is a leading cause of death in patients. Mutations to the dystrophin gene result in myocyte membrane instability, contributing to the structural deterioration of the diaphragm muscle tissues. With previous works suggesting the importance of lipin1 for maintaining skeletal muscle membrane integrity, we explored the roles of lipin1 in the dystrophic diaphragm. We found that the protein expression levels of lipin1 were reduced by 60% in the dystrophic diaphragm. While further knockdown of lipin1 in the dystrophic diaphragm leads to increased necroptosis, restoration of lipin1 in the dystrophic diaphragm results in reduced inflammation and fibrosis, decreased myofiber death, and improved respiratory function. Our results demonstrated that lipin1 restoration improved respiratory function by enhancing membrane integrity and suggested that lipin1 could be a potential therapeutic target for preventing respiratory insufficiency and respiratory failure in DMD. Continued investigation is required to better understand the mechanisms behind these findings, and to determine the role of lipin1 in maintaining muscle membrane stability.

KEYWORDS

lipin1, DMD, muscular dystrophy, dystrophin, diaphragm, skeletal muscle, therapeutic target, membrane integrity

Background

Duchenne muscular dystrophy (DMD) is an X-linked recessive disorder that is characterized by severe and progressive muscle weakness and muscle wasting including respiratory muscles (Duan et al., 2021). This disease is caused by a mutation in the largest known human gene which encodes the protein, dystrophin. Dystrophin is a cytoskeletal protein connecting the inner cytoskeleton to the extracellular matrix and

Abbreviations: DMD, Duchenne muscular dystrophy; EBD, Evans blue dye; PA, phosphatidic acid; PAP, phosphatidic acid phosphatase; DAG, diacylglycerol; WT, wild-type; RIPK, receptor-interacting serine/threonine-protein kinase; MLKL, mixed-lineage kinase domain-like protein; OCT, optimal cutting temperature; WT, wildtype; MCK, muscle creatine kinase; CK, creative kinase.

serves as a molecular shock absorber to maintain sarcolemmal stability and protect the muscles from injury (Le et al., 2018). Dystrophin deficiency leads to impairment of skeletal muscle sarcolemmal membrane integrity, including the diaphragm, rendering the membrane susceptible to mechanical damage during muscle contraction, leading to immune cell infiltration, necrosis, and fibrosis (Bez Batti Angulski et al., 2023). These histopathological abnormalities of the respiratory muscle have been shown to lead to reduced lung and chest wall compliance, decreased ventilation, and alveolar hypoventilation in many boys with DMD (Smith et al., 1989; Barbe et al., 1994). Patients with DMD have reduced ventilatory capacity beginning at a young age and will decline with age (Burns et al., 2019; Khirani et al., 2014). Respiratory insufficiency is ubiquitous in patients at older age and respiratory failure is one of the leading causes of morbidity and mortality in muscular dystrophy, with a mean life expectancy between 14.4 and 27.0 years unless artificially supported by mechanical ventilation (Pennati et al., 2021; Landfeldt et al., 2020).

A primary strategy to treat DMD would be to reverse the instability of muscle membranes by increasing dystrophin levels. However, a major obstacle to that approach is that the dystrophin gene is too large to be packaged into current gene therapy vectors. While Elevidys micro-dystrophin gene therapy has recently been approved by FDA, these highly truncated forms of dystrophin do not offer full protection (Elangkovan and Dickson, 2021). Moreover, exon-skipping therapies including Amondys 45, Exondys 51, Viltespo, and Vyondys 53 are only effective for some dystrophin mutations (Eser and Topaloglu, 2022). Therefore, it is critical to identify new molecules that are important for ameliorating dystrophic phenotypes and restoring diaphragm function in DMD.

Lipin1 is a phosphatidic acid (PA) phosphatase (PAP) that catalyzes the conversion of PA into diacylglycerol (DAG), which is a critical step in the synthesis of glycerophospholipids, the major structural lipid component of cellular membranes (Csaki and Reue, 2010). Lipin1 accounts for most of the PAP activity in skeletal muscles (Reue and Dwyer, 2009). We recently discovered that lipin1 is critical for maintaining membrane integrity, and plays complementary roles in myofiber stability and muscle function in dystrophic skeletal muscles (Jama et al., 2023). Lipin1 deficiency in skeletal muscle led to membrane damage indicated by increased Evans blue dye (EBD) leakage (Ramani et al., 2020; Schweitzer et al., 2019). Increased membrane permeability was associated with elevated cell death markers and inflammation. This is consistent with our cell culture study, lipin1 deficiency in differentiated primary myoblasts leads to increased membrane permeability and upregulated necroptotic markers (Jama et al., 2023). In contrast, increasing lipin1 expression levels suppressed the necroptotic markers (Jama et al., 2023).

In this study, we aimed to explore the role of lipin1 in dystrophic pathogenesis and respiratory dysfunction through loss-of-function and gain-of-function studies in the *mdx* mouse diaphragm. We assessed the effects of knocking out lipin1 in dystrophic diaphragm histology and function using *dystrophin:lipin1-DKO* mice, and the effects of restoring lipin1 in dystrophic diaphragm using a unique muscle-specific transgenic mouse model, *mdx:lipin1^{Tg/0}*, in which lipin1 is selectively restored in the muscles of *mdx* mice. We found that *DKO* mice had increased dystrophic disease severity, whereas increasing lipin1 expression levels led to decreased muscle fiber degeneration, suppressed

inflammation, reduced fibrosis, strengthened membrane integrity, and improved respiratory function.

Methods

Animals

Skeletal muscle-specific lipin1 deficient (*lipin1^{Myf5cKO}*) mice were generated by crossing lipin1^{fl/fl} with mice expressing Cre recombinase driven by Myf5 promoter as described in our previous study (Jama et al., 2024). C57BL/10ScSnJ (B10, #000476) *WT* and *mdx* (#001801) mice were originally purchased from Jackson Laboratories (Bar Harbor, ME, United States). *Dystrophin/lipin1-DKO* mice were generated by crossing *lipin1^{Myf5cKO}* with *mdx* mice as described in our previous study (Jama et al., 2023). Hemizygous *mdx:lipin1^{Tg/0}* mice were generated by crossing *mdx* mice with muscle-specific lipin1 transgenic mice generated by crossing Rosa26-Stop-Lipin1 knockin (Rosa26-lipin1^{KI}) mice with mice carrying the Cre recombinase driven by the muscle creatine kinase (MCK) gene promoter (Jama et al., 2024). Because DMD occurs primarily in males, male mice at 6–7 months of age were used in the present study. These mice had free access to drinking water and regular chow unless otherwise noted. All animal experiments were performed in accordance with the relevant guidelines and regulations approved by the Animal Care and Use Committee of Wright State University and approval was obtained for all experiments performed in the present study.

Western blotting

As described in our previous studies (Jiang et al., 2015; Alshudukhi et al., 2018), diaphragm muscle tissues were homogenized using RIPA buffer containing 10 mM Tris-HCl (pH 8.0), 30 mM NaCl, 1 mM EDTA, and 1% Nonidet P-40, supplemented with proteinase inhibitors and phosphatase inhibitors before use. Protein concentration was determined for each sample by BCA assay to ensure that equal amounts of protein were used across all samples. The samples were boiled for 5 min with 4x loading dye and separated by 7.5%–15% SDS-PAGE. Proteins were transferred to polyvinylidene difluoride membranes (Millipore) using a Mini Trans-Blot Cell System (Bio-Rad). The membrane was blocked with 5% nonfat milk (9999; Cell Signaling Technologies) for 1 h, and incubated with the primary antibodies in 5% BSA (BP9704; Thermo Fisher Scientific) in TBST overnight at 4°C. After probing with secondary antibodies for 1 h at room temperature, protein bands were detected by using Amersham Imager 600 (GE Healthcare Life Sciences). GAPDH (Cell Signaling Technologies, dilution 1:5000, catalog 2118) antibody was used as a loading control. The primary antibodies from Cell Signaling Technology were used, at dilution 1:1000, include lipin1 (catalog 4906), RIPK3 (catalog 95702), RIPK1 (catalog 3493), MLKL (catalog 37705), Cleaved Caspase-3 (catalog 9664), SMAD2/3 (catalog 8685), pSMAD2 serine 465/567 (catalog 3108), NF-κB (catalog 8242), pNF-κB serine 468 (catalog 3039), pNF-κB serine 536 (catalog 3033), Bax (catalog 2772), and Bak (catalog 12105). The NIH ImageJ software was used to quantify all western blots by densitometry. The values obtained were normalized to the loading control.

Evans blue dye (EBD) assay

Mice were injected with EBD (10 mg/mL stock in sterile saline, 0.1 mL/10 g body weight) by i.p. and euthanized 24 h later. The skeletal muscles were dissected and snap-frozen in isopentane-cooled optimal cutting temperature (OCT) embedding media (Tissue-Tek, Sakura-Americas). Frozen OCT blocks were cryosectioned at 10 μ m thickness and stained with laminin antibody before being analyzed by fluorescence microscopy.

Immunofluorescence, microscopy, and image processing

The diaphragm muscles were frozen and sectioned at 10 μ m using a cryostat machine. Slides were stored at -20°C . For staining, muscle sections were air dried for 1 h at room temperature. The muscle sections were then hydrated with PBST, followed by blocking with 5% goat serum in PBST. To detect macrophage distribution, sections were incubated with antibodies against CD86 (Abcam, catalog ab239075, dilution 1:100), CD206 (Cell Signaling Technology, catalog 24595, dilution 1:1000), or laminin (Abcam, catalog ab11575, dilution 1:500) for 1 h at 37°C , and subsequently with an Alexa Fluor 488-conjugated secondary antibody (Thermo Fisher Scientific, catalog A-21411, dilution 1:250) for 1 h in the dark at room temperature. Images were obtained using an inverted microscope (Olympus, IX70) equipped with a DFC7000T camera (Leica Microsystems, Wetzlar, Germany). Indicated images were quantified by CellProfiler software (Brown et al., 2023).

Respiratory function analysis

Respiratory function assay was performed using whole-body plethysmography (FinePointe; Buxco/DSI) in conscious, unrestrained animals. Pressure sensor calibration was achieved via direct injection of a 5 mL bolus of air into the experimental chamber and was automated by computer software. Animals were acclimatized to the plethysmography chamber (BUXCO Europe Ltd.) for 3 days before experiments. On the day of the experiments, animals were introduced into plethysmography chambers and allowed a 20-min acclimation period with constant flow (200 mL/min) of compressed air to prevent the buildup of CO_2 and depletion of O_2 . Following the acclimation period, respiratory parameters including respiratory frequency (F), tidal volume (TV), and minute ventilation (MV) were recorded over a 10-min interval. These measurements were averaged by the system software (FinePointe v2.3.1.16; Buxco/DSI) and imported into Microsoft Excel for statistical analysis.

Statistical analysis

For immunostaining and Western blotting, statistical analysis was performed by one-way analysis of variance (ANOVA) followed by Bonferroni's multiple comparison test to determine significant changes between groups using Prism, version 9.4.0 (GraphPad Software Inc., San Diego, CA, United States). Data are reported as

the mean \pm SD and the number (n) of independent experiments. For ANOVA analyses, a *p*-value of less than 0.05 was considered significant.

Results

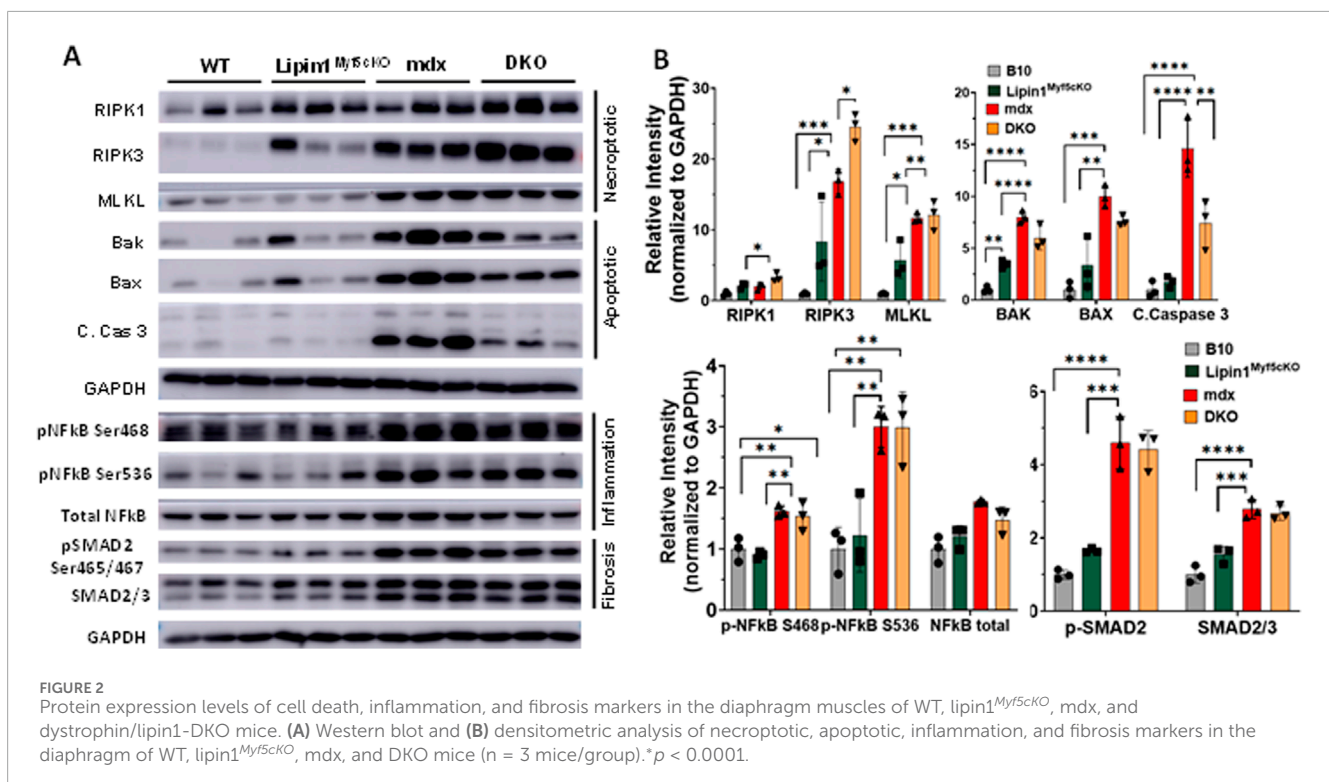
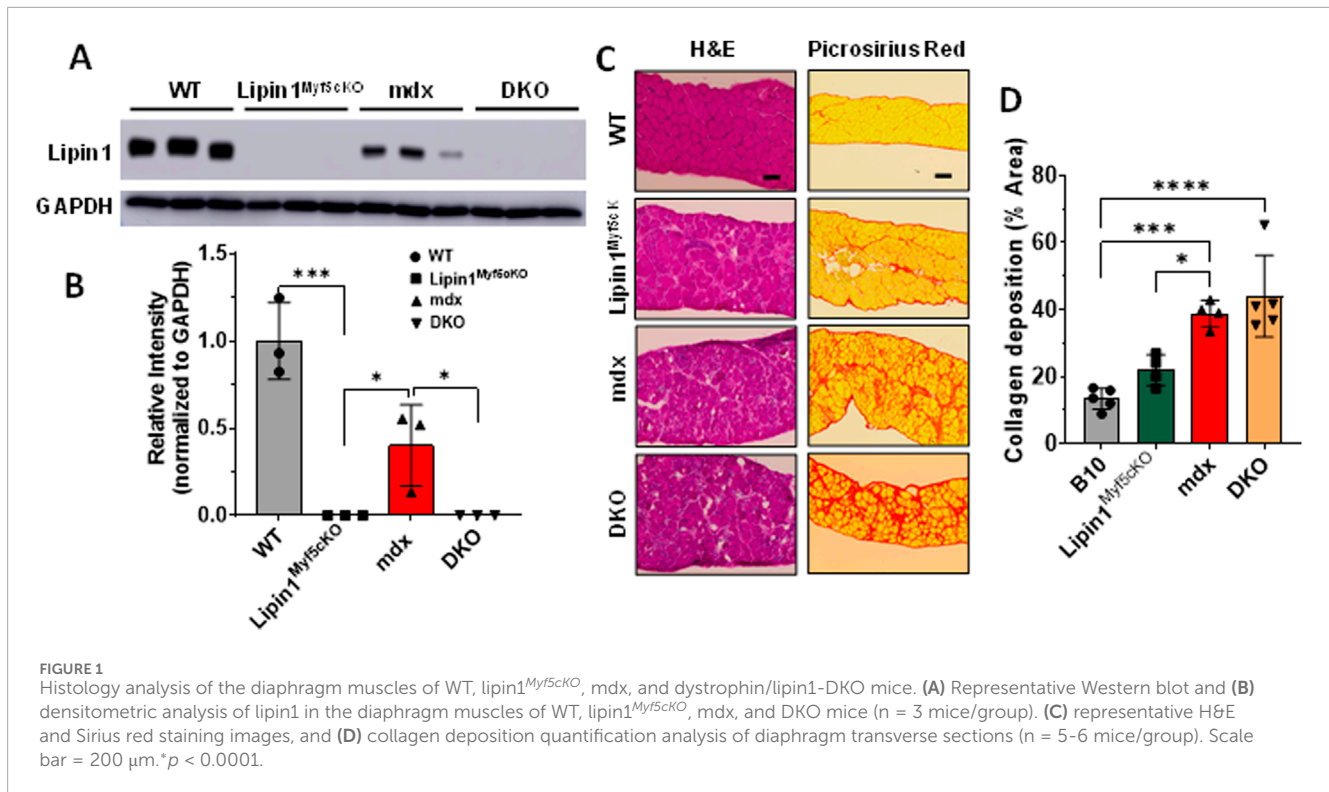
Further knockout of lipin1 in dystrophic diaphragm worsens diaphragm histopathology

To assess the role of lipin1 in dystrophic diaphragm muscle, we employed *dystrophin:lipin1-DKO* (DKO) mouse model (Jama et al., 2023). The protein expression levels of lipin1 in the diaphragm of 6-month-old B10 wildtype (WT), skeletal muscle-specific lipin1 knockout (*lipin1^{Myf5cKO}*), *mdx*, and *DKO* mice were measured by Western blotting. While the *lipin1^{Myf5cKO}* and *DKO* mice did not show any lipin1 expression, the *mdx* diaphragm exhibited a 60% reduction of lipin1 expression compared to the WT diaphragm ($p = 0.007$, Figures 1A,B), which is consistent with our previous study (Jama et al., 2023). We compared the histopathological changes in the diaphragm of WT, *lipin1^{Myf5cKO}*, *mdx*, and *DKO* mice at 6 months of age. Hematoxylin and eosin (H&E) staining revealed mild inflammation infiltration and fibrosis in *lipin1^{Myf5cKO}* mice, but some areas along the *mdx* and *DKO* mouse diaphragm cross-section were completely overridden by pale fibrotic tissue (Figure 1C).

As increased fibrosis results in elevated muscle stiffness and contributes to respiratory failure, we also evaluated fibrosis in *mdx* and *DKO* mice at 6 months old using Picosirius red staining. In comparison to the WT diaphragm, the *lipin1^{Myf5cKO}* diaphragm presented a 60% increase in collagen deposition. Collagen deposition was further exacerbated in the *mdx* and *DKO* diaphragm, which showed nearly a 2.9- and 3.2-fold increase ($p = 0.0005$ and $p < 0.0001$), respectively in comparison to the WT diaphragm (Figures 1C,D).

Further knockout of lipin1 in the dystrophic diaphragm leads to enhanced cell death, inflammation, and fibrosis

Necroptosis, a form of regulated necrotic cell death, is mediated by receptor-interacting serine/threonine-protein kinase 1 (RIPK1), RIPK3, and mixed-lineage kinase-domain-like pseudokinase (MLKL) which contribute to muscle degeneration (Morgan et al., 2018). In DMD, RIPK3 is thought to be the major driver of limb muscle degeneration (Morgan et al., 2018). To identify the role of lipin1 overexpression in diaphragm muscle degeneration, we assessed these necroptosis markers in the diaphragm of 6-month-old B10 WT, *lipin1^{Myf5cKO}*, *mdx*, and *DKO* mice (Figures 2A,B). We found that RIPK1 and RIPK3 were significantly increased by 2- and 16-fold ($p = 0.025$ and $p = 0.001$) respectively, in *mdx* and further increased by 3- and 25-fold ($p = 0.0005$ and $p < 0.0001$) respectively in *DKO* compared to the WT diaphragm (Figures 2A,B). Although necroptotic markers were elevated in the *dystrophin:lipin1-DKO* diaphragm compared to the *mdx* diaphragm, we did not find significant differences in apoptotic cell death markers between these two groups. It is likely that necroptosis rather than apoptosis is the



main cell death pathway contributing to the tissue damage observed by further knockdown of lipin1.

NF- κ B is a master transcriptional factor regulating inflammation response. Phosphorylation of NF- κ B at Ser468 and

Ser536 has been shown to stimulate NF- κ B transcriptional activity (Viator et al., 2005; Campbell and Perkins, 2004; Oeckinghaus et al., 2011). We found that both Ser468 and Ser536 of NF- κ B were highly increased in the *mdx* ($p = 0.005$ and $p = 0.004$) and *DKO*

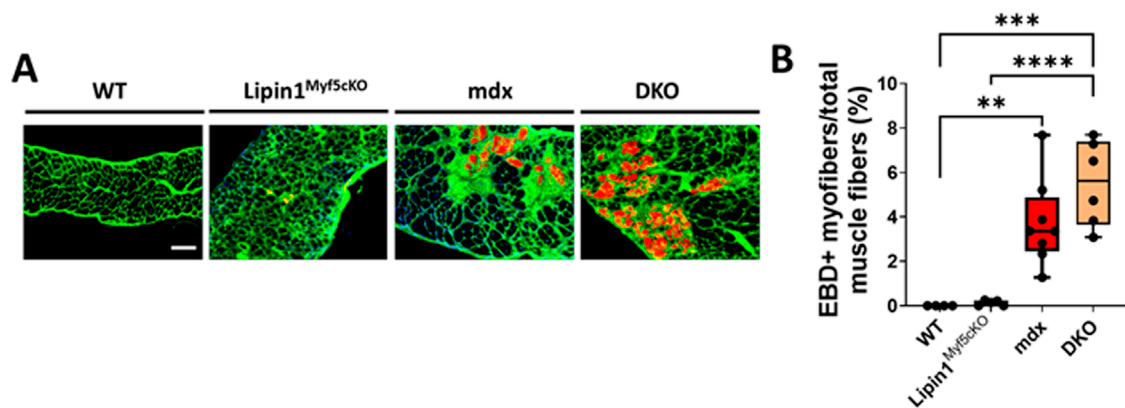


FIGURE 3

Muscle damage in the diaphragms of WT, *lipin1^{Myf5cKO}*, *mdx*, and dystrophin/*lipin1*-DKO mice. **(A)** Representative images of EBD uptake (red) in diaphragm muscle sections of WT, *lipin1^{Myf5cKO}*, *mdx*, and DKO mice. WGA (green) was used to visualize the borders of muscle fibers and DAPI (blue) stained nuclei. **(B)** Quantification analysis of EBD-positive muscle fiber expressed as the percentage of the total number of muscle fibers in each mouse ($n = 4-8$ mice/group). Scale bar = 200 μm . ** $p < 0.01$; *** $p < 0.001$; **** $p < 0.0001$.

($p = 0.011$ and $p = 0.004$) diaphragms compared to the WT diaphragm (Figures 2A,B). We did not find a further activation of NF- κ B in the DKO diaphragm compared to the *mdx* diaphragm. Since increased SMAD signaling has been shown to drive the expression of extracellular matrix components such as collagens (Walton et al., 2017), we measured the protein expression levels of SMAD2/3 and found that protein expression levels were elevated by 2.7-fold in *mdx* and DKO diaphragms compared to WT diaphragm ($p < 0.0001$). Phosphorylation of SMAD2 at Ser465 and Ser467 promotes SMAD activation (Souchelnytskyi et al., 1997). Phospho-SMAD2 was also substantially elevated in *mdx* and DKO diaphragms compared to WT controls ($p < 0.0001$ and $p < 0.0001$, respectively). We did not observe any difference in protein expression levels of SMAD2/3 and pSMAD2 between the *mdx* and DKO diaphragms.

To determine whether knockout of *lipin1* affects diaphragm muscle damage in *mdx* mice, we injected EBD into WT, *lipin1^{Myf5cKO}*, *mdx*, and DKO mice. Compared to WT controls, muscle damage was observed in both *mdx* and DKO diaphragms, but we did not observe any difference in muscle damage between *mdx* and DKO diaphragms (Figure 3). Wheat germ agglutinin (WGA) staining was used to identify the myofiber borders.

Restoration of *lipin1* in *mdx:lipin1^{Tg/0}* mice prevented pathology of the dystrophic diaphragm

To evaluate whether increasing *lipin1* expression levels in dystrophic diaphragm could suppress dystrophic pathology, we generated mice with *lipin1* specifically overexpressed in skeletal muscles (*Rosa26-lipin1^{K1}*) by crossing *Rosa26-Stop-Lipin1* mice with mice carrying the Cre recombinase driven by the MCK gene promoter. We further crossed *Rosa26-lipin1^{K1}* with *mdx* mice, and generated *mdx:lipin1* transgenic mice (*mdx:lipin1^{Tg/0}*) in which *lipin1* was selectively increased in the dystrophic muscles of *mdx* mice, including in the diaphragm. We found that protein expression levels of *lipin1* were substantially reduced in the diaphragm of

mdx mice ($p = 0.007$, Figures 4A,B). Whereas, increasing *lipin1* in hemizygous *mdx:lipin1^{Tg/0}* mice restored *lipin1* expression to its physiological levels similar to WT controls. Thus, hemizygous *mdx:lipin1^{Tg/0}* mice have been used to examine the effect of *lipin1* overexpression on DMD pathogenesis.

Muscle morphology analysis using H&E staining revealed decreased tissue damage in the *lipin1*-restored dystrophic diaphragm (Figure 4C). We also evaluated fibrosis in *mdx* and *mdx:lipin1^{Tg/0}* mice at 6 months using Picrosirius red staining (Figures 4C,D). In comparison to the *mdx* diaphragm, the *mdx:lipin1^{Tg/0}* diaphragm appeared to display substantially reduced fibrosis ($p = 0.0008$).

Restoration of *lipin1* in the dystrophic diaphragm suppressed cell death, inflammation, and fibrosis

To identify the role of *lipin1* overexpression in diaphragm muscle degeneration, we assessed necroptotic markers in the diaphragm of 6-month-old hemizygous *mdx:lipin1^{Tg/0}* and their *mdx* controls. As shown in Figures 5A,B, the expression levels of RIPK1, RIPK3, and MLKL were significantly elevated by 590%, 470%, and 310% ($p < 0.0001$, $p < 0.0001$, and $p = 0.005$) respectively in the *mdx* diaphragm compared to WT controls, but reduced to 26%, 41%, and 66% ($p = 0.0001$, $p < 0.0001$, and $p = 0.034$) respectively in the diaphragm of *mdx:lipin1^{Tg/0}* compared to *mdx* mice, suggesting that increasing *lipin1* expression levels inhibits necroptosis. The apoptotic markers BAK ($p = 0.02$), and cleaved-caspase-3 ($p = 0.004$) were elevated in the *mdx* diaphragm. However, restoration of *lipin1* in dystrophic diaphragm did not reduce their expression levels compared to *mdx* diaphragm (Figure 5B) suggesting that restoration of *lipin1* prevented the activation of necroptotic markers rather than apoptotic markers in dystrophic muscle.

Activation of NF- κ B was measured to evaluate the effects of increasing *lipin1* expression levels on inflammation in the dystrophic diaphragm. Western blot analysis showed that

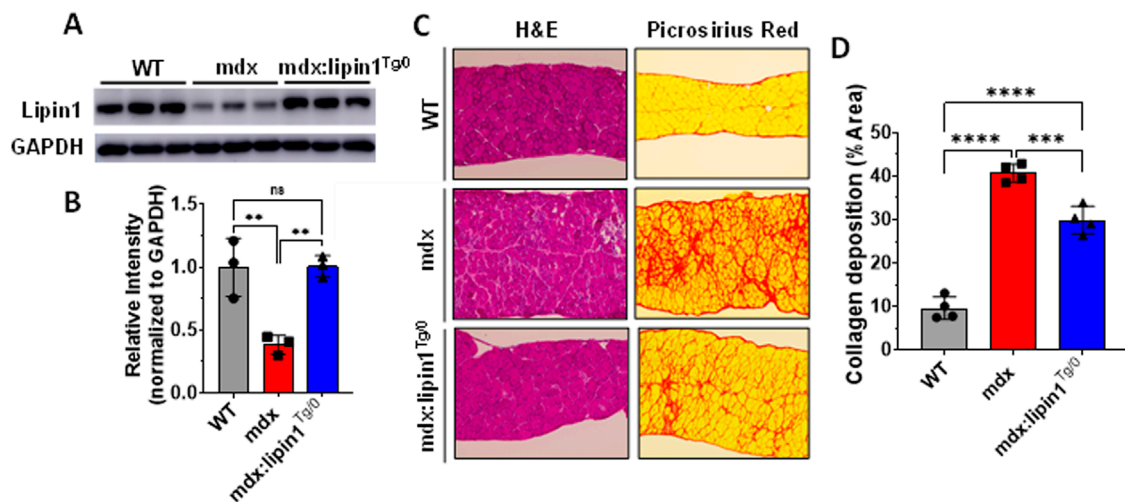


FIGURE 4 Histology analysis of the diaphragm muscles of WT, mdx, and mdx:lipin1^{Tg0} mice. **(A)** Representative Western blot and **(B)** densitometric analysis of lipin1 in the diaphragm muscles of WT, mdx, and mdx:lipin1^{Tg0} mice ($n = 3$ mice/group). **(C)** Representative H&E and Sirius red staining images, and **(D)** collagen deposition quantification analysis of diaphragm transverse sections ($n = 4-5$ mice/group). Scale bar = 200 μm . ** $p < 0.01$; *** $p < 0.001$; **** $p < 0.0001$.

phosphorylation of NF- κB at serine 468 and 536 was elevated ($p = 0.0114$ and $p = 0.0031$, respectively) in the diaphragm muscle of mdx compared to *B10* WT mice but was reduced to 59% and 55% ($p = 0.04$ and $p = 0.006$), respectively, in mdx:lipin1^{Tg0} compared to mdx mice (Figures 5A,B). Phosphorylation of SMAD2 was elevated by 420% in the mdx diaphragm and was reduced to 60% ($p = 0.0421$) when the expression of lipin1 was restored. Altogether this data suggests that restoration of lipin1 expression in the dystrophic diaphragm reduces cell death and inflammation, which ultimately leads to decreased collagen accumulation.

To further evaluate whether restoration of lipin1 could prevent inflammation, we also evaluated inflammatory macrophage distribution in *B10*, mdx, and mdx:lipin1^{Tg0} mice using immunohistochemistry. CD86⁺ macrophages are proinflammatory M1 macrophages that play an important role in dystrophic muscle pathology (Mojumdar et al., 2014). CD206⁺ macrophages are M2 macrophages that promote fibrosis development (Coulis et al., 2023). The abundance and distribution of CD86⁺ and CD206⁺ macrophages were detected by immunostaining in *B10*, mdx, and mdx:lipin1^{Tg0} muscle (Figures 5C,D). The surface area per cross-sectional area of CD86⁺ M1 macrophage was increased to 2.3% ($p = 0.0005$) in mdx compared to WT muscle, but was reduced to 1.0% ($p = 0.01$) in mdx:lipin1^{Tg0} muscle (Figure 5C). Moreover, CD206⁺ M2 macrophage was increased to 4.8% ($p = 0.0001$) in mdx compared to 0.1% in WT muscle, but was reduced to 0.96% ($p = 0.0005$) in mdx:lipin1^{Tg0} compared to mdx muscle (Figure 5D).

Restoration of lipin1 reduced diaphragm muscle damage

To determine whether restoration of lipin1 level alleviates muscle damage in mdx mice, we injected EBD into WT, mdx, and mdx:lipin1^{Tg0} mice. Compared to mdx littermates,

mdx:lipin1^{Tg0} mice had much fewer EBD-positive muscle fibers ($p = 0.03$, Figure 6), suggesting that lipin1 upregulation increased sarcolemma stability and reduced muscle damage in mdx mice. These results suggest that compromised membrane integrity in dystrophic skeletal muscle can be ameliorated by lipin1 upregulation.

Further knockout of lipin1 in the dystrophic diaphragm impaired respiratory function, and restoration of lipin1 improved respiratory function

Respiratory failure is a leading cause of death in DMD patients (Walton et al., 2017). Using whole-body plethysmography, we measured respiratory function in conscious, unrestrained 6-month-old WT, lipin1^{Myf5cKO}, mdx, DKO, and mdx:lipin1^{Tg0} mice. In the absence of just lipin1 in the lipin1^{Myf5cKO} mice, we did not observe any statistically significant respiratory impairment in comparison to the *B10* WT mice (Figures 7A–C). We found that mdx mice had reduced respiratory rate ($p < 0.0001$, Figure 7A), and minute volume ($p = 0.0003$, Figure 7C) compared to WT mice, as in previous studies (Huang et al., 2011; Burns et al., 2015). Further knockout of lipin1 in dystrophic muscle led to a significantly reduced respiratory rate from 356 breaths/min to 344 breaths/min ($p = 0.01$, Figures 7A–C). The difference in tidal volume change between mdx mice and WT mice did not reach significance possibly due to sample variation, but the average tidal volume was reduced in mdx mice, which is consistent with a previous finding (Huang et al., 2011). There was not a significant difference in the tidal volumes and minute volumes between the mdx and dystrophin/lipin1-DKO mice most likely because mdx mice already present low levels of lipin1. In contrast, respiratory rate, and minute volume were all significantly improved in mdx:lipin1^{Tg0} compared

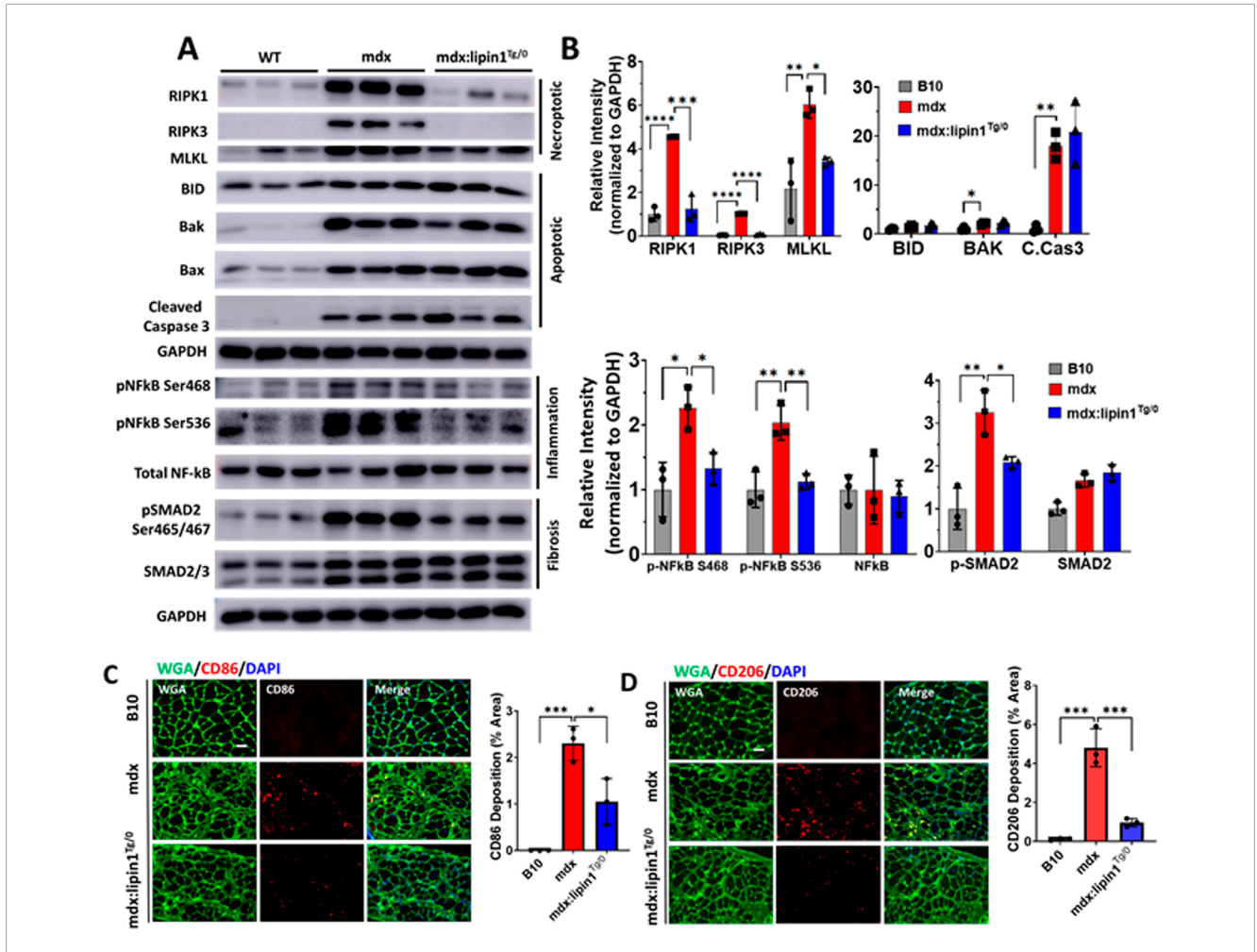


FIGURE 5 Protein expression levels of cell death, inflammation, and fibrosis markers in the diaphragm muscles of WT, mdx, and mdx:lipin1^{Tg/0} mice. (A) Western blot and (B) quantification analysis of necroptotic, apoptotic, inflammatory, and fibrosis markers in the diaphragm of WT, mdx, and mdx:lipin1^{Tg/0} mice. Representative immunostaining of (C) CD86+ (red) and (D) CD206+ (red) macrophages in diaphragms of indicated mice. WGA (green) was used to visualize the borders of muscle fibers and DAPI (blue) stained nuclei. Scale bar = 100 μm. n = 3 mice/group. *p < 0.05 **p < 0.01; ***p < 0.001; ****p < 0.0001.

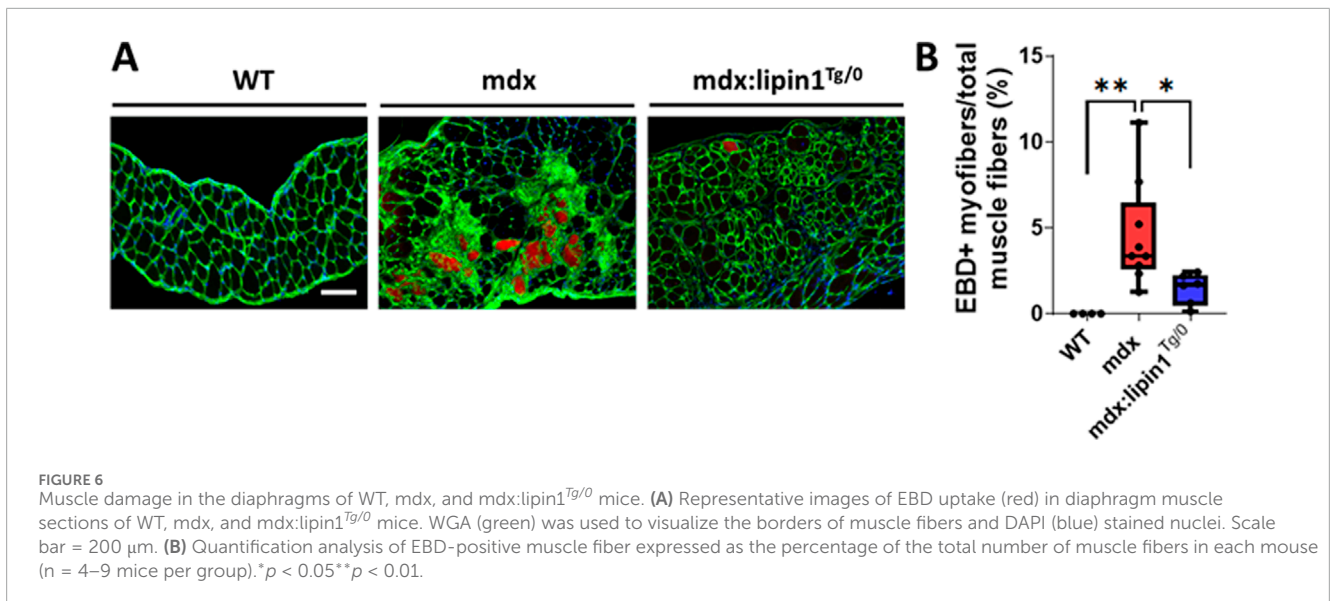


FIGURE 6 Muscle damage in the diaphragms of WT, mdx, and mdx:lipin1^{Tg/0} mice. (A) Representative images of EBD uptake (red) in diaphragm muscle sections of WT, mdx, and mdx:lipin1^{Tg/0} mice. WGA (green) was used to visualize the borders of muscle fibers and DAPI (blue) stained nuclei. Scale bar = 200 μm. (B) Quantification analysis of EBD-positive muscle fiber expressed as the percentage of the total number of muscle fibers in each mouse (n = 4–9 mice per group). *p < 0.05 **p < 0.01.

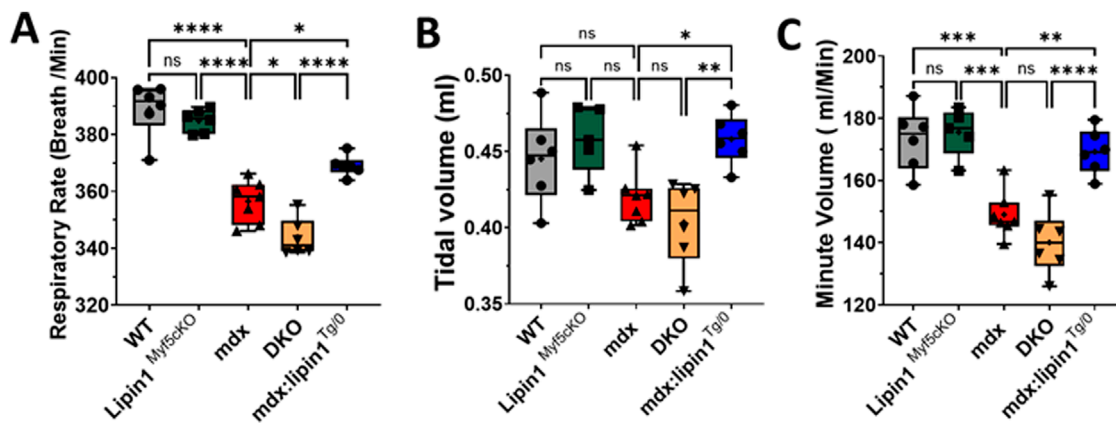


FIGURE 7 Respiratory function measurement of WT, *lipin1^{Myf5cko}*, *mdx*, DKO, and *mdx:lipin1^{Tg/0}* mice. (A) Respiratory rate, (B) tidal volume, and (C) minute volume in WT, *lipin1^{Myf5cko}*, *mdx*, DKO, and *mdx:lipin1^{Tg/0}* mice. All were measured by whole-body plethysmography. Respiratory measurements were taken over a 10-minute interval and averaged to obtain the data points for each mouse ($n = 6-7$ mice per group). * $p < 0.05$; ** $p < 0.01$; *** $p < 0.001$; **** $p < 0.0001$.

to *mdx* mice ($p = 0.002$, Figures 7A–C), suggesting that increasing *lipin1* expression levels improved respiratory function.

Discussion

Respiratory failure is a leading cause of premature death in DMD patients. Although respiratory malfunction in DMD patients is slightly alleviated by noninvasive mechanical ventilation, identifying therapeutic targets and improving respiratory function would greatly impact DMD patients' quality of life. In this study, we explored the roles of *lipin1* in the dystrophic diaphragm and respiratory function using loss-of-function and gain-of-function approaches.

We identified that *lipin1* protein expression levels were reduced by 60% in the *mdx* diaphragm. This is consistent with our previous study, which found that *lipin1* decreased by 60% in the *mdx* gastrocnemius muscle compared to WT controls (Jama et al., 2023). Our recent studies revealed that *lipin1* plays a complementary role in myofiber stability and muscle function in dystrophic muscles (Jama et al., 2023; Ramani et al., 2020; Jama et al., 2024). *Lipin1* deficiency alone leads to compromised plasma membrane integrity, elevated necroptotic markers, and inflammation (Jama et al., 2023; Ramani et al., 2020). It is possible that *lipin1* expression levels were already very low, so, further knockout of the remaining 40% of *lipin1* in the dystrophic diaphragm did not lead to a significant worsening phenotype in this study. However, we did find that NF- κ B, a master transcriptional factor of inflammation, was highly activated in the *mdx* and DKO diaphragms as indicated by enhanced phosphorylation of NF- κ B at serine 468 and serine 536.

Dystrophin deficiency leads to an increase in muscle damage. The imbalance between muscle damage and repair is associated with apoptotic and necrotic cell death contributing to muscle fiber loss. Previous studies suggested that apoptosis characterizes the onset of the pathology of dystrophin-deficient muscle and

precedes necrosis (Tidball et al., 1995). Apoptosis has been identified by nuclei with DNA fragmentation in the muscles of DMD patients and *mdx* mice (Tidball et al., 1995; Matsuda et al., 1995; Sandri and Carraro, 1999). Necroptosis, programmed necrosis, is distinguished from other modes of cell death in that it is highly proinflammatory given that cell membrane integrity is lost, triggering the activation of the immune system and inflammation. Therefore, necroptosis has been shown to be a major contributor to muscle degeneration in dystrophic muscles contributing to the loss of muscle fibers (Oeckinghaus et al., 2011). In our study, highly elevated Bax, Bak, and cleaved caspase 3 may indicate elevated apoptotic death in the *mdx* diaphragm. We observed that RIPK1, RIPK3, and MLKL are elevated in the diaphragm muscle of *mdx* mice, and RIPK1 and RIPK3 are further upregulated in the DKO diaphragm. Elevated necroptosis is not the only mechanism leading to muscle degeneration. Sarcolemmal disruptions, abnormal calcium (Ca^{2+}) homeostasis (Culligan et al., 2002; Doran et al., 2006; Matsumura et al., 2009), increased calpain activities (Spencer and Mellgren, 2002), and NF- κ B³⁸ have been shown to contribute to muscle degeneration. The effects of loss of *lipin1* in Ca^{2+} homeostasis and calpain activities remain to be investigated. Nevertheless, as a result of increased muscle degeneration, loss of *lipin1* in the dystrophic diaphragm may lead to deterioration of respiratory function, indicated by a decrease in respiratory rate, which represents the most sensitive indicator of increasing respiratory difficulty.

Given the fact that loss of *lipin1* plays an important role in dystrophic pathology, increasing *lipin1* expression levels may have resulted in an improvement in muscle membrane integrity and respiratory function in *mdx* mice. Indeed, we found that the diaphragm of *mdx:lipin1^{Tg/0}* mice had fewer EBD-positive muscle fibers compared to *mdx* controls, suggesting that compromised membrane integrity in the dystrophic diaphragm can be ameliorated by *lipin1* restoration. This is consistent with our recent studies that *lipin1* deficiency leads to increased sarcolemmal permeability, increased creatine kinase (CK) levels, and elevated necroptotic

markers in animal models and cell culture systems (Jama et al., 2023; Jama et al., 2024). On the contrary, restoration of lipin1 in dystrophic muscle resulted in reduced sarcolemmal permeability, reduced serum CK levels, and downregulated necroptotic markers. Furthermore, restoration of lipin1 rescued the protein expression levels of α -sarcoglycan, dystroglycan, and nNOS, and promoted sarcolemmal stability (Jama et al., 2024).

Inflammation and cell death are effective hallmarks of membrane instability and dystrophin deficiency in DMD. NF- κ B transcriptional activity is progressively elevated in DMD, and has been shown to contribute to disease onset and progression (Messina et al., 2011). We observed that the phosphorylation of NF- κ B at serine 468 and serine 536 was suppressed in the diaphragm of *mdx:lipin1^{Tg/0}* mice. In addition, CD86⁺ and CD206⁺ macrophages were highly elevated in *mdx* and DKO diaphragms compared to B10 controls suggesting that lipin1 restoration in dystrophic diaphragm significantly reduces myofiber inflammation. The protein expression levels of RIPK1, RIPK3, and MLKL were significantly suppressed in the diaphragm of *mdx:lipin1^{Tg/0}* mice, suggesting that lipin1 restoration in dystrophic diaphragm reduced myofiber necrosis. Either inhibition of cell death or inflammation has been shown to improve dystrophic phenotype. Corticosteroids have been the first-line anti-inflammatory drugs approved by the FDA for the treatment of DMD. Inhibition of NF- κ B in cardiomyocytes improved calcium handling and rescued cardiac function (Peterson et al., 2018). Genetic or pharmacologic inhibition of classical NF- κ B DNA-binding subunit, p65, or its upstream activator, I κ B kinase β (IKK β), have been found to reduce inflammation and improve muscle regeneration in *mdx* mice (Acharyya et al., 2007). Genetic depletion of RIPK3 in dystrophic *mdx* mice reduced muscle degeneration and improved motor function (Morgan et al., 2018).

The ensuing loss of myofibers, largely mediated by a necrotic cell death process, is associated with the progressive replacement of the myofibers by fibrosis. Overall, our data suggest that the *mdx* diaphragm showed enhanced fibrosis indicated by Sirius red staining and activation of SMAD2. Activation of SMAD signaling via the canonical TGF β pathway has been shown to promote collagen deposition and fibrosis (Coulis et al., 2023). Elevated diaphragm fibrosis results in muscle stiffness, prevents the diaphragm from achieving the excursion lengths required for respiration, and is the major contributor to the disease progression (Sahani et al., 1985). Increasing lipin1 expression in dystrophic muscle leads to substantially suppressed SMAD activation and reduced fibrosis development in *mdx:lipin1^{Tg/0}* mice.

Patients with DMD experience progressive respiratory muscle weakness by 10–12 years of age (Spencer and Mellgren, 2002; Kumar and Boriek, 2003). As DMD progresses to later stages, patients often present a significant increase in respiratory rate, which is known as rapid shallow breathing (Lo Mauro and Aliverti, 2016). It has been suggested that rapid shallow breathing is adopted as a strategy to reduce the perception of labored breathing (Lo Mauro and Aliverti, 2016). We found that the respiratory rates, tidal volume, and minute volume were reduced in *mdx* and *mdx:lipin1-DKO* mice at 6 months of age measured by plethysmography. This is consistent with previous studies that *mdx* mice at 6 months old had significantly impaired respiratory function, indicated by reduced respiratory frequency, tidal volume, and minute volume (Huang et al., 2011). The impaired respiratory function is likely due to increased

diaphragm sarcolemmal damage, inflammation, elevated cell death, and increased fibrosis which confer mechanical defects in the *mdx* diaphragm. We also found that restoration of lipin1 in the dystrophic diaphragm significantly improved the respiratory rate, tidal volume, and minute volume, suggesting that increasing lipin1 levels successfully improved respiratory function in *mdx* mice.

It should be noted that we observed only 4% of EBD⁺ myofibers in the skeletal muscle of *mdx* mice. The ratio was calculated by EBD⁺ myofiber areas versus the total muscle fiber area. The total muscle fiber areas were calculated by measuring the areas of the diaphragm ruling out the tissue gaps between borders of myofibers (Brown et al., 2023; Dubuisson et al., 2022). However, the amount of muscle damage does not seem to match the degree of impaired respiratory function and elevated cell death, inflammation, and fibrosis markers. These results suggest that the EBD staining may not represent muscle damage, but muscle sarcolemmal leakage. Although dystrophin-deficient muscle cells are vulnerable to membrane damage, not all muscle damage leads to sarcolemmal leakage when subjected to increased mechanical stress. Therefore, EBD staining needs to be combined with other techniques, such as plasma creatine kinase levels (Jama et al., 2023; Kobayashi et al., 2012), and the identification of intracellular fibronectin in muscle cells (Friden and Lieber, 1998) to provide a more comprehensive and integrated view of muscle damage. Indeed, in our recent study (Jama et al., 2024), we observed that *mdx* mice had elevated CK levels and increasing lipin1 expression levels in *mdx:lipin1^{Tg/0}* mice reduced CK levels suggesting a critical role for lipin1 in maintaining myofiber stability and integrity. Another reason that leads to low EBD⁺ myofibers in 6-month-old *mdx* mice may be due to age. Previous studies found that EBD is significantly more abundant in the diaphragm of 4-week-old *mdx* than in the diaphragm of 24-week-old *mdx* mice (Pelosi et al., 2015). It is possible that younger *mdx* mice may exhibit more damaged muscle fibers. The variations of sarcolemmal leakage in *mdx* mice affected by age will need to be investigated in the future.

In conclusion, we found that lipin1 expression level is markedly reduced in the *mdx* diaphragm. Loss of lipin1 is associated with increased severity of pathology in the dystrophic diaphragm and contributes to respiratory dysfunction. In contrast, lipin1 overexpression significantly improves the primary defect and downstream pathology in the dystrophic diaphragm, resulting in improved membrane integrity, prevented inflammation, decreased muscle fiber degeneration, reduced fibrosis, and most importantly, improved respiratory function. These findings suggest that lipin1 is an important therapeutic target in the management and treatment of respiratory insufficiency and failure in DMD. In future studies, more functional assays will be introduced to highlight the protective effects of lipin1 on respiratory muscles. We will conduct *ex vivo* contractile assessments to measure the isometric force production of a thin diaphragm muscle strip. We will conduct exercise testing (e.g., running wheel; treadmill) on the *mdx:lipin1^{Tg/0}*, *mdx:mdx:lipin1-DKO*, and *mdx* mice. This type of stress will provide interesting discrimination from a whole-body functional perspective if lipin1 is overexpressed versus reduced in the *mdx* diaphragm. We will also assess whether lipin1 overexpression can ameliorate functional impairments and cellular markers of damage in a more severe mouse model (e.g., *D2.mdx* or *mdx-utrn dKO* mice). To explore the potential of lipin1 overexpression for treating respiratory failure,

we will use an AAV-based strategy as a therapeutic tool to efficiently deliver lipin1 to the diaphragm. We will investigate the effectiveness, possible adverse effects, and long-term safety of different expression levels of lipin1 as a potential therapy for respiratory dysfunction in DMD. Another future direction is to investigate if older aged mice also present rapid shallow breathing with the progression of the disease; and if lipin1 restoration could help to mitigate this response. Moreover, continued investigation is required to better understand the mechanisms behind these findings, and to determine the role of lipin1 in maintaining muscle membrane stability.

Data availability statement

The datasets used and/or analyzed during the current study are available from the corresponding author upon reasonable request and directed to Hongmei Ren, hongmei.ren@wright.edu.

Ethics statement

The animal study was approved by Animal Care and Use Committee of Wright State University. The study was conducted in accordance with the local legislation and institutional requirements.

Author contributions

AB: Data curation, Formal Analysis, Methodology, Validation, Visualization, Writing–review and editing. BM: Data curation, Formal Analysis, Validation, Visualization, Writing–review and editing, Methodology. JK: Data curation, Formal Analysis, Validation, Visualization, Writing–review and editing, Methodology. RR: Writing–review and editing, Resources, Methodology, Validation. BF: Funding acquisition, Writing–review and editing, Resources, Validation. CW: Writing–review and editing, Resources, Validation. HR: Conceptualization, Data

References

- Acharyya, S., Villalta, S. A., Bakkar, N., Bupha-Intr, T., Janssen, P. M., Carathers, M., et al. (2007). Interplay of IKK/NF-kappaB signaling in macrophages and myofibers promotes muscle degeneration in Duchenne muscular dystrophy. *J. Clin. Invest.* 117 (4), 889–901. doi:10.1172/JCI30556
- Alshudukhi, A. A., Zhu, J., Huang, D. T., Jama, A., Smith, J. D., Wang, Q. J., et al. (2018). Lipin-1 regulates Bnip3-mediated mitophagy in glycolytic muscle. *Faseb J.* 32 (12), 6796–6807. doi:10.1096/fj.201800374
- Barbe, F., Quera-Salva, M. A., McCann, C., Gajdos, P., Raphael, J. C., de Lattre, J., et al. (1994). Sleep-related respiratory disturbances in patients with Duchenne muscular dystrophy. *Eur. Respir. J.* 7 (8), 1403–1408. doi:10.1183/09031936.94.07081403
- Bez Batti Angulski, A., Hosny, N., Cohen, H., Martin, A. A., Hahn, D., Bauer, J., et al. (2023). Duchenne muscular dystrophy: disease mechanism and therapeutic strategies. *Front. Physiol.* 14, 1183101. PMID: 10330733. doi:10.3389/fphys.2023.1183101
- Brown, A., Morris, B., Kaumau, J. K., Alshudukhi, A. A., Jam, A., and Ren, H. (2023). Automated image analysis pipeline development to monitor disease progression in muscular dystrophy using cell profiler. *Arch. Microbiol. Immunol.* 7 (1), 178–187. doi:10.26502/ami.936500115
- Burns, D. P., Edge, D., O'Malley, D., and O'Halloran, K. D. (2015). Respiratory control in the mdx mouse model of Duchenne muscular dystrophy. *Adv. Exp. Med. Biol.* 860, 239–244. doi:10.1007/978-3-319-18440-1_27
- Burns, D. P., Murphy, K. H., Lucking, E. F., and O'Halloran, K. D. (2019). Inspiratory pressure-generating capacity is preserved during ventilatory and non-ventilatory behaviours in young dystrophic mdx mice despite profound diaphragm muscle weakness. *J. Physiology-London* 597 (3), 831–848. doi:10.1113/JP277443
- Campbell, K. J., and Perkins, N. D. (2004). Post-translational modification of RelA(p65) NF-kappaB. *Biochem. Soc. Trans.* 32 (Pt 6), 1087–1089. doi:10.1042/BST0321087
- Coulis, G., Jaime, D., Guerrero-Juarez, C., Kastenschmidt, J. M., Farahat, P. K., Nguyen, Q., et al. (2023). Single-cell and spatial transcriptomics identify a macrophage population associated with skeletal muscle fibrosis. *Sci. Adv.* 9 (27), eadd9984. doi:10.1126/sciadv.add9984
- Csaki, L. S., and Reue, K. (2010). Lipins: multifunctional lipid metabolism proteins. *Annu. Rev. Nutr.* 30, 257–272. doi:10.1146/annurev.nutr.012809.104729
- Culligan, K., Banville, N., Dowling, P., and Ohlendieck, K. (2002). Drastic reduction of calsequestrin-like proteins and impaired calcium binding in dystrophic mdx muscle. *J. Appl. Physiology* 92 (2), 435–445. doi:10.1152/jappphysiol.00903.2001
- Doran, P., Dowling, P., Donoghue, P., Buffini, M., and Ohlendieck, K. (2006). Reduced expression of regucalcin in young and aged mdx diaphragm indicates abnormal cytosolic calcium handling in dystrophin-deficient muscle. *Biochim. Biophys. Acta* 1764 (4), 773–785. doi:10.1016/j.bbapap.2006.01.007

curation, Funding acquisition, Investigation, Methodology, Project administration, Resources, Supervision, Validation, Writing–original draft, Writing–review and editing.

Funding

The author(s) declare that financial support was received for the research, authorship, and/or publication of this article. This project was supported by an NIH grant (5R01 AR077574) and DoD Idea Development Award (W81XWH2110679) awarded to HR. The generation of lipin1 overexpressing mice was supported by R01 HL119225 to BF.

Conflict of interest

The authors declare that the research was conducted in the absence of any commercial or financial relationships that could be construed as a potential conflict of interest.

Publisher's note

All claims expressed in this article are solely those of the authors and do not necessarily represent those of their affiliated organizations, or those of the publisher, the editors and the reviewers. Any product that may be evaluated in this article, or claim that may be made by its manufacturer, is not guaranteed or endorsed by the publisher.

Supplementary material

The Supplementary Material for this article can be found online at: <https://www.frontiersin.org/articles/10.3389/fphys.2024.1477976/full#supplementary-material>

- Duan, D., Goemans, N., Takeda, S., Mercuri, E., and Aartsma-Rus, A. (2021). Duchenne muscular dystrophy. *Nat. Rev. Dis. Prim.* 7 (1), 13. doi:10.1038/s41572-021-00248-3
- Dubuisson, N., Versele, R., Planchon, C., Selvais, C. M., Noel, L., Abou-Samra, M., et al. (2022). Histological methods to assess skeletal muscle degeneration and regeneration in Duchenne muscular dystrophy. *Int. J. Mol. Sci.* 23 (24), 16080. doi:10.3390/ijms232416080
- Elangkovan, N., and Dickson, G. (2021). Gene therapy for Duchenne muscular dystrophy. *J. Neuromuscul. Dis.* 8, S303–S316. doi:10.3233/JND-210678
- Eser, G., and Topaloglu, H. (2022). Current outline of exon skipping trials in Duchenne muscular dystrophy. *Genes (Basel)* 13 (7), 1241. doi:10.3390/genes13071241
- Friden, J., and Lieber, R. L. (1998). Segmental muscle fiber lesions after repetitive eccentric contractions. *Cell. Tissue Res.* 293 (1), 165–171. doi:10.1007/s004410051108
- Huang, P., Cheng, G., Lu, H. Y., Aronica, M., Ransohoff, R. M., and Zhou, L. (2011). Impaired respiratory function in mdx and mdx/Utrn^{+/−} mice. *Muscle and Nerve* 43 (2), 263–267. doi:10.1002/mus.21848
- Jama, A., Alshudukhi, A. A., Burke, S., Dong, L., Kamau, J. K., Morris, B., et al. (2024). Exploring lipin1 as a promising therapeutic target for the treatment of Duchenne muscular dystrophy. *J. Transl. Med.* 22 (1), 664. doi:10.1186/s12967-024-05494-z
- Jama, A., Alshudukhi, A. A., Burke, S., Dong, L., Kamau, J. K., Voss, A. A., et al. (2023). Lipin1 plays complementary roles in myofiber stability and regeneration in dystrophic muscles. *J. Physiol.* 601 (5), 961–978. doi:10.1113/JP284085
- Jiang, W. H., Zhu, J., Zhuang, X., Zhang, X. P., Luo, T., Esser, K. A., et al. (2015). Lipin1 regulates skeletal muscle differentiation through extracellular signal-regulated kinase (ERK) activation and cyclin D complex-regulated cell cycle withdrawal. *J. Biol. Chem.* 290 (39), 23646–23655. doi:10.1074/jbc.M115.686519
- Khirani, S., Ramirez, A., Aubertin, G., Boule, M., Chemouny, C., Forin, V., et al. (2014). Respiratory muscle decline in Duchenne muscular dystrophy. *Pediatr. Pulmonol.* 49 (5), 473–481. doi:10.1002/ppul.22847
- Kobayashi, Y. M., Rader, E. P., Crawford, R. W., and Campbell, K. P. (2012). Endpoint measures in the mdx mouse relevant for muscular dystrophy pre-clinical studies. *Neuromuscul. Disord.* 22 (1), 34–42. doi:10.1016/j.nmd.2011.08.001
- Kumar, A., and Boriek, A. M. (2003). Mechanical stress activates the nuclear factor-kappaB pathway in skeletal muscle fibers: a possible role in Duchenne muscular dystrophy. *FASEB J.* 17 (3), 386–396. doi:10.1096/fj.02-0542com
- Landfeldt, E., Thompson, R., Sejersen, T., McMillan, H. J., Kirschner, J., and Lochmüller, H. (2020). Life expectancy at birth in Duchenne muscular dystrophy: a systematic review and meta-analysis. *Eur. J. Epidemiol.* 35 (7), 643–653. doi:10.1007/s10654-020-00613-8
- Le, S., Yu, M., Hovan, L., Zhao, Z., Ervasti, J., and Yan, J. (2018). Dystrophin as a molecular shock absorber. *ACS Nano* 12 (12), 12140–12148. PMID: 6632074. doi:10.1021/acsnano.8b05721
- Lo Mauro, A., and Aliverti, A. (2016). Physiology of respiratory disturbances in muscular dystrophies. *Breathe (Sheff.)* 12 (4), 318–327. doi:10.1183/20734735.012716
- Matsuda, R., Nishikawa, A., and Tanaka, H. (1995). Visualization of dystrophic muscle fibers in mdx mouse by vital staining with Evans blue: evidence of apoptosis in dystrophin-deficient muscle. *J. Biochem.* 118 (5), 959–964. doi:10.1093/jb/118.5.959
- Matsumura, C. Y., Pertille, A., Albuquerque, T. C., Santo Neto, H., and Marques, M. J. (2009). Diltiazem and verapamil protect dystrophin-deficient muscle fibers of MDX mice from degeneration: a potential role in calcium buffering and sarcolemmal stability. *Muscle Nerve* 39 (2), 167–176. doi:10.1002/mus.21188
- Messina, S., Vita, G. L., Aguenouz, M., Sframeli, M., Romeo, S., Rodolico, C., et al. (2011). Activation of NF-kappaB pathway in Duchenne muscular dystrophy: relation to age. *Acta Myol.* 30 (1), 16–23.
- Mojumdar, K., Liang, F., Giordano, C., Lemaire, C., Danialou, G., Okazaki, T., et al. (2014). Inflammatory monocytes promote progression of Duchenne muscular dystrophy and can be therapeutically targeted via CCR2. *EMBO Mol. Med.* 6 (11), 1476–1492. doi:10.15252/emmm.201403967
- Morgan, J. E., Prola, A., Mariot, V., Pini, V., Meng, J., Hourde, C., et al. (2018). Necroptosis mediates myofiber death in dystrophin-deficient mice. *Nat. Commun.* 9 (1), 3655. doi:10.1038/s41467-018-06057-9
- Oeckinghaus, A., Hayden, M. S., and Ghosh, S. (2011). Crosstalk in NF-κB signaling pathways. *Nat. Immunol.* 12 (8), 695–708. doi:10.1038/ni.2065
- Pelosi, L., Berardinelli, M. G., Forcina, L., Spelta, E., Rizzuto, E., Nicoletti, C., et al. (2015). Increased levels of interleukin-6 exacerbate the dystrophic phenotype in mdx mice. *Hum. Mol. Genet.* 24 (21), 6041–6053. doi:10.1093/hmg/ddv323
- Pennati, F., LoMauro, A., D'Angelo, M. G., and Aliverti, A. (2021). Non-invasive respiratory assessment in Duchenne muscular dystrophy: from clinical research to outcome measures. *Life (Basel)* 11 (9), 8468718. doi:10.3390/life11090947
- Peterson, J. M., Wang, D. J., Shettigar, V., Roof, S. R., Canan, B. D., Bakkar, N., et al. (2018). NF-κB inhibition rescues cardiac function by remodeling calcium genes in a Duchenne muscular dystrophy model. *Nat. Commun.* 9 (1), 3431. doi:10.1038/s41467-018-05910-1
- Ramani, S. S., Jama, A., Alshudukhi, A. A., Townsend, N. E., Miranda, D. R., Reese, R. R., et al. (2020). Loss of membrane integrity drives myofiber death in lipin1-deficient skeletal muscle. *Physiol. Rep.* 8 (8), e14620. doi:10.14814/phy2.14620
- Reue, K., and Dwyer, J. R. (2009). Lipin proteins and metabolic homeostasis. *J. Lipid Res.* 50, 109–114. doi:10.1194/jlr.R800052-JLR200
- Sahani, R., Wallace, C. H., Jones, B. K., and Blemker, S. S. (1985). Diaphragm muscle fibrosis involves changes in collagen organization with mechanical implications in Duchenne muscular dystrophy. *J. Appl. Physiol.* 132 (3), 653–672. doi:10.1152/jappphysiol.00248.2021
- Sandri, M., and Carraro, U. (1999). Apoptosis of skeletal muscles during development and disease. *Int. J. Biochem. Cell. Biol.* 31 (12), 1373–1390. doi:10.1016/s1357-2725(99)00063-1
- Schweitzer, G. G., Collier, S. L., Chen, Z., McCommis, K. S., Pittman, S. K., Yoshino, J., et al. (2019). Loss of lipin 1-mediated phosphatidic acid phosphohydrolase activity in muscle leads to skeletal myopathy in mice. *FASEB J.* 33 (1), 652–667. doi:10.1096/fj.201800361R
- Smith, P. E., Edwards, R. H., and Calverley, P. M. (1989). Ventilation and breathing pattern during sleep in Duchenne muscular dystrophy. *Chest* 96 (6), 1346–1351. doi:10.1378/chest.96.6.1346
- Souchelnytskyi, S., Tamaki, K., Engstrom, U., Wernstedt, C., ten Dijke, P., and Heldin, C. H. (1997). Phosphorylation of Ser465 and Ser467 in the C terminus of Smad2 mediates interaction with Smad4 and is required for transforming growth factor-beta signaling. *J. Biol. Chem.* 272 (44), 28107–28115. doi:10.1074/jbc.272.44.28107
- Spencer, M. J., and Mellgren, R. L. (2002). Overexpression of a calpastatin transgene in mdx muscle reduces dystrophic pathology. *Hum. Mol. Genet.* 11 (21), 2645–2655. doi:10.1093/hmg/11.21.2645
- Tidball, J. G., Albrecht, D. E., Lokensgard, B. E., and Spencer, M. J. (1995). Apoptosis precedes necrosis of dystrophin-deficient muscle. *J. Cell. Sci.* 108 (Pt 6), 2197–2204. doi:10.1242/jcs.108.6.2197
- Viatour, P., Merville, M. P., Bours, V., and Chariot, A. (2005). Phosphorylation of NF-kappaB and IkappaB proteins: implications in cancer and inflammation. *Trends Biochem. Sci.* 30 (1), 43–52. doi:10.1016/j.tibs.2004.11.009
- Walton, K. L., Johnson, K. E., and Harrison, C. A. (2017). Targeting TGF-β mediated SMAD signaling for the prevention of fibrosis. *Front. Pharmacol.* 8, 461. PMID: 5509761. doi:10.3389/fphar.2017.00461